Vietnam Journal of Science and Technology ***57*** *(6A) (2019) 150-160*

doi:10.15625/2525-2518/57/6A/14655

SOUND TRANSMISSION LOSS ACROSS A FINITE CLAMPED DOUBLE-LAMINATED COMPOSITE PLATE WITH POROELASTIC MATERIAL

Pham Ngoc Thanh[1, *], Tran Ich Thinh[2]

[1]*Viettri University of Industry, Street Hung Vuong, Viet Tri, Phu Tho, Viet Nam*

[2]*Hanoi University of Science and Technology, 1 Dai Co Viet, Hai Ba Trung, Ha Noi, Viet Nam*

[*]Email: *thanhpham1986@gmail.com*

Received: 28 November 2019; Accepted for publication: 25 December 2019

Abstract. A theoretical study of sound transmission loss across a clamped double-laminated composite plate filled with poroelastic material is formulated. Biot's theory is employed to describe wave propagation in elastic porous media. The two face composite plates are modeled as classical thin plates. By using the modal superposition theory, a double series solution for the sound transmission loss of the structure is obtained with the help of the Galerkin method. The analytical model is validated against previous experimental results of a single sound wave under normal incidence. The numerical results suggest that the density of poroelastic material, the type of composite materials and the composite plies arrangement have significant effects on the sound transmission loss of considered structure.

Keywords: composite sandwich plate, double-composite plate, porous material, sound transmission loss, sound insulation.

Classification numbers: 2.9.4, 5.4.5.

1. INTRODUCTION

Double-wall sandwich plates are widely used in many modern industrial fields due to their superior insulation and mechanical properties over a wide frequency range compared to many other devices such as their single-wall counterparts.

There is extensive literature considering the problem of sound transmission through double-plates of infinite lateral dimensions. Bolton *et al*. [1] used Biot's theory [2] on wave propagation in a poroelastic medium to evaluate sound transmission loss through infinite double-metallic plates filled with porous materials, and have validated the theoretical model developed against their experimental results. Lee *et al*. [3] modified Bolton's model by neglecting the shear wave and only considering the energetically strongest wave among those propagating in the porous material and. However, only few researchers have attempted to solve the problem of finite sandwich plates. To study the effect of finite extent, boundary effects must be taken into account. If studies on simple boundary conditions attracted slightly more attention [4, 5], only

little work has been done on clamped boundary conditions. Xin and Lu [6] have paved the way by investigated both analytically and experimentally sound transmission loss through clamped and simply supported double-plates containing an air cavity but without any absorptive core. Up to now, no research efforts have been made to the vibroacoustic problem of sound transmission through clamped double-composite plates filled with a porous material. The aim of the present work is hence to develop an analytical model to address this problem by combining the approach of Lu and Xin [7] and the model of Bolton *et al*. on sandwich panels with poroelastic cores [1]. Thanh and Thinh [8] studied vibro-acoustic of a finite orthotropic laminated double-composite plate with enclosed air cavity using the acoustic velocity potential to describe the acoustic vibration performance of a simple supported structure. Approach of Panneton *et al*. [9] applied to the sound transmission loss through multilayer structures made from a combination of elastic, air, and poroelastic materials. Their mode is based on a three-dimensional finite element model. It uses classical elastic and fluid elements to model the elastic and fluid media. For the poroelastic material, it uses a two-field displacement formulation derived from the Biot theory.

The present study has expanded a model to calculate the sound transmission across a finite clamped laminated double-composite plate with poroelastic material. The effect of several key system parameters on STL of this composite structure (e.g., the type of composite materials, the composite plies arrangement and effect of density of porous material) is systematically examined.

2. THOERETICAL FORMULATION

A double-laminated composite plate lined with poroelastic materials consists of two rectangular, orthotropic, homogeneous and sufficiently thin plates commonly made of laminated composite, as illustrated in Fig. 1. The two elastic plates are fully clamped along their edges to an infinite rigid acoustic baffle. This double-composite plate is filled with porous materials. The bottom plate is excited by a plane harmonic sound wave with ω being the angular frequency and the symbol $j = \sqrt{-1}$. Without loss of generality, an incident sound wave of unit amplitude is assumed, and its incident direction is determined by the elevation angle φ and the azimuth angle θ (see Fig. 1).

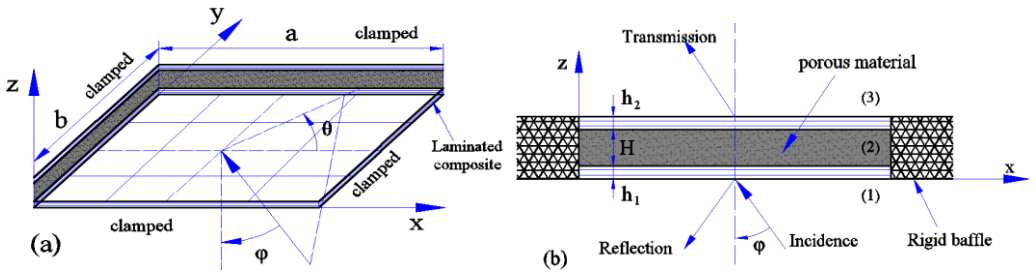

Figure 1. Schematic of a clamped double- laminated composite plate lined with poroelastic materials: (a) global view, (b) side view.

The vibrations of the upper plate are transmitted through the structure via the poroelastic medium to the bottom plate which induces pressure variations and thus a transmitted sound wave. The incidence field and transmission field separated by the infinite rigid baffle are assumed to be semi-infinite with identical air properties, i.e. air density ρ_0 and speed of sound in

ambient air c_0. The panel dimensions are chosen as follows: *a; b* are the length and width of the plate, h_1; h_2 are the thicknesses of the bottom and upper plates, and *H* is the total thickness of the sandwich core (porous materials) in between the two plates.

2.1. Wave propagation in poroelastic medium

According to Biot's theory [2], an elastic porous material is assumed statistically isotropic and has the solid phase (elastic frame) as well as the fluid phase (air contained in pores). The model of Bolton [1] allows three waves in the porous material, two longitudinal waves, and one shear wave. Meanwhile, Lee *et al*. [3] shown that the shear wave is always negligible compared to the longitudinal waves. Hence, there are four wave components within the porous material, i.e. positive and negative propagating components of the two most energetically waves along the *z*-axis, which are characterized by the complex amplitudes D_1-D_4. Thus, the displacements of the solid and fluid phase are obtained as [1]:

$$u_z^s = je^{-j\left(k_x x+k_y y-\omega t\right)}\left(D_1\frac{k_{1z}}{k_1^2}e^{-jk_{1z}z}-D_2\frac{k_{1z}}{k_1^2}e^{jk_{1z}z}+D_3\frac{k_{2z}}{k_2^2}e^{-jk_{2z}z}-D_4\frac{k_{2z}}{k_2^2}e^{jk_{2z}z}\right) \quad (1)$$

$$u_z^f = je^{-j\left(k_x x+k_y y-\omega t\right)}\left(c_1D_1\frac{k_{1z}}{k_1^2}e^{-jk_{1z}z}-c_1D_2\frac{k_{1z}}{k_1^2}e^{jk_{1z}z}+c_2D_3\frac{k_{2z}}{k_2^2}e^{-jk_{2z}z}-c_2D_4\frac{k_{2z}}{k_2^2}e^{jk_{2z}z}\right) \quad (2)$$

The normal stresses in the *z*-direction are determined by [1]:

$$\sigma_z^s = e^{-j\left(k_x x+k_y y-\omega t\right)}\left[\varepsilon_1^s\left(D_1e^{-jk_{1z}z}+D_2e^{jk_{1z}z}\right)+\varepsilon_2^s\left(D_3e^{-jk_{2z}z}+D_4e^{jk_{2z}z}\right)\right] \quad (3)$$

$$\sigma_z^f = e^{-j\left(k_x x+k_y y-\omega t\right)}\left[\varepsilon_1^f\left(D_1e^{-jk_{1z}z}+D_2e^{jk_{1z}z}\right)+\varepsilon_2^f\left(D_3e^{-jk_{2z}z}+D_4e^{jk_{2z}z}\right)\right] \quad (4)$$

where the parameters $\varepsilon_1^s, \varepsilon_2^s, \varepsilon_1^f, \varepsilon_2^f$ are defined by:

$$\begin{aligned}&\varepsilon_1^s = 2N\frac{k_{1z}^2}{k_1^2}+A+c_1Q, \qquad \varepsilon_2^s = 2N\frac{k_{2z}^2}{k_2^2}+A+c_2Q\\ &\varepsilon_1^f = Q+c_1S, \qquad \varepsilon_2^f = Q+c_2S\end{aligned} \quad (5)$$

and

$$\begin{aligned}&c_1 = b_1-b_2k_1^2, c_2 = b_1-b_2k_2^2; b_1 = \left(\rho_{11}^*S-\rho_{12}^*Q\right)/\left(\rho_{22}^*Q-\rho_{12}^*S\right); b_2 = \left(PS-Q^2\right)/\left[\omega^2\left(\rho_{22}^*Q-\rho_{12}^*S\right)\right]\\ &A = \frac{\nu_s E_s}{\left(1+\nu_s\right)\left(1-2\nu_s\right)}; \quad N = \frac{E_s}{2\left(1+\nu_s\right)}; \quad Q = \left(1-\beta\right)E_f; \quad S = \beta E_f\end{aligned} \quad (6)$$

where the wavenumbers, k_1^2, k_2^2, and the complex equivalent densities, ρ_{ij} (*i, j =1, 2*) are detailed in [1]. E_s is the static Young's modulus of solid phase; ν_s is the Poision's ratio and E_f denotes the bulk modulus of the fluid in the pores; β is the porosity of the porous material.

Four constants, D_1 - D_4, in Eqs. (1) - (4) can be determined by applying boundary conditions at the plate-air-lining interface:
At

$$z = h_1, \quad -\frac{\partial \Phi_1}{\partial z} = j\omega w_1, \quad u_z^s = w_1, \; u_z^f = w_1 \tag{7}$$

at

$$z = H + h_1 \quad -\frac{\partial \Phi_3}{\partial z} = j\omega w_2, \quad u_z^s = w_2, \; u_z^f = w_2 \tag{8}$$

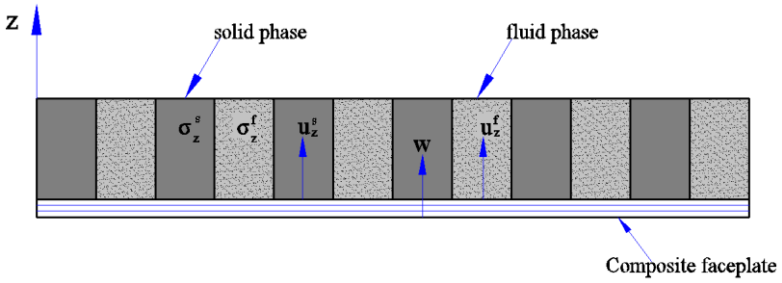

Figure 2. Cross-sectional view of porous layer attached to the face composite plate.

2.2. Wave Propagation through laminated composites

The vibro-acoustic response of an orthotropic symmetric composite double-plate with poroelastic materials (Fig. 1) induced by sound excitation is governed by [7, 8]:

$$D_{11}\frac{\partial^4 w_1(x,y;t)}{\partial x^4} + 2(D_{12}+2D_{66})\frac{\partial^4 w_1(x,y;t)}{\partial x^2 \partial y^2} + D_{22}\frac{\partial^4 w_1(x,y;t)}{\partial y^4} + m_1^*\frac{\partial^2 w_1}{\partial t^2} = j\omega\rho_0\Phi_1 + \sigma_z^s + \sigma_z^f \tag{9}$$

$$D_{11}\frac{\partial^4 w_2(x,y;t)}{\partial x^4} + 2(D_{12}+2D_{66})\frac{\partial^4 w_2(x,y;t)}{\partial x^2 \partial y^2} + D_{22}\frac{\partial^4 w_2(x,y;t)}{\partial y^4} + m_2^*\frac{\partial^2 w_2}{\partial t^2} = -j\omega\rho_0\Phi_3 - \sigma_z^s - \sigma_z^f \tag{10}$$

where: w_1, w_2 are the transverse displacements of the upper and bottom plates, respectively. $m_i^* = \rho_p h_i (i = 1,2)$ is the mass per unit area of the upper and bottom plates; ρ_p is the density of the upper or bottom plates; ρ_0 is the density of air; Φ_1 and Φ_3 are the acoustic velocity potential in the incident sound field and the transmission field; D_{ij} is the flexural rigidity:

$$D_{ij} = \frac{1}{3}\sum_{k=1}^{n} Q_{ij}^k \left(z_{k+1}^3 - z_k^3\right) \tag{11}$$

Note that, for an isotropic plate, $D_{11} = D_{22} = Eh^3/[12(1-\nu^2)]$, $D_{12} = \nu D_{11}$, $D_{66} = Gh^3/12$.

Under the excitation of harmonic sound waves, the transverse deflection of the upper and bottom composite plates can be expressed in a form of modal decomposition:

$$w_1(x,y,t) = \sum_{m,n} \varphi_{mn}(x,y)\alpha_{1,mn} e^{j\omega t}; \quad w_2(x,y,t) = \sum_{m,n} \varphi_{mn}(x,y)\alpha_{2,mn} e^{j\omega t} \tag{12}$$

For the clamped boundary, the modal functions take the form [7, 10]:

$$\varphi_{mn}(x,y) = \left(1 - \cos\frac{2m\pi x}{a}\right)\left(1 - \cos\frac{2n\pi y}{b}\right) \tag{13}$$

and $\alpha_{1,mn}$; $\alpha_{2,mn}$ are the modal coefficients of the plate displacement and will be determined by applying the following clamped boundary conditions:

$$x = 0, a, \forall\, 0 < \mathrm{y} < \mathrm{b},\ \mathrm{w}_1 = w_2 = 0,\ \frac{\partial \mathrm{w}_1}{\partial \mathrm{x}} = \frac{\partial w_2}{\partial x} = 0 \tag{14}$$

$$y = 0, b, \forall\, 0 < \mathrm{x} < \mathrm{a},\ \mathrm{w}_1 = w_2 = 0,\ \frac{\partial \mathrm{w}_1}{\partial \mathrm{y}} = \frac{\partial w_2}{\partial y} = 0 \tag{15}$$

The acoustic velocity potential in the incident sound field (field 1 in Fig.1) consists of an incident wave and a reflective wave with the amplitudes I and β, respectively, and it can be expressed in a harmonic form as [7]:

$$\Phi_1 = Ie^{-j\left(k_x x + k_y y + k_z z - \omega t\right)} + \beta e^{-j\left(k_x x + k_y y - k_z z - \omega t\right)} \tag{16}$$

where a unit amplitudes has been assumed for the incident wave, i.e. $I = 1$.

The transmission field (field 3 in Fig. 1) with the amplitude γ in this field and its velocity potential can be written as [7]:

$$\Phi_3 = \gamma e^{-j\left(k_x x + k_y y + k_z z - \omega t\right)} \tag{17}$$

The sound power of the incident or transmitted wave per unit area (i.e. acoustic intensity) is defined as $p = \mathrm{Re}\left(pv^*\right)/2$, and the acoustic particle velocity is related to the sound pressure through $p = p/\left(\rho_0 c_0\right)$ for harmonic waves. The sound power can be expressed as [7]:

$$\Pi = \frac{1}{2} Re \int_0^b \int_0^a p v_z^* dA = \frac{1}{2\rho_0 c_0} \int_0^b \int_0^a p^2 dA \tag{18}$$

These acoustic velocity potentials are related to the acoustic pressure p and the normal acoustic particle velocity v_z^* in the fluid and solid field [8, 11]:

$$p = \rho_0 \frac{\partial \Phi}{\partial t} = j\omega \rho_0 \Phi; \quad v_z^* = -\frac{\partial \Phi}{\partial z} \tag{19}$$

Considering the relation (19) and the velocity potential definitions (16) and (17), the sound power of incident and transmitted are determined by [7, 8]

$$\Pi_1 = \frac{\omega^2 \rho_0}{2c_0} \int_0^b \int_0^a \Phi_1^2 dxdy; \qquad \Pi_3 = \frac{\omega^2 \rho_0}{2c_0} \int_0^b \int_0^a \Phi_3^2 dxdy \tag{20}$$

The sound transmission loss (STL) is calculated in decibel scale via [7]

$$STL(\varphi, \theta) = 10 \log\left[1/\tau\left(\varphi, \theta\right)\right] \tag{21}$$

where τ is the transmission coefficient and is defined as the ratio of the transmitted and incident sound power by [8, 10]

$$\tau\left(\varphi, \theta\right) = \frac{\Pi_3}{\Pi_1} \tag{22}$$

In order to determine the unknown $\alpha_{1,mn}$ and $\alpha_{2,mn}$, applying the Galerkin method to the plate motion equations (9) and (10) leads to

$$\int_0^b \int_0^a \left(\begin{array}{l} D_{11} \dfrac{\partial^4 w_1(x,y;t)}{\partial x^4} + 2(D_{12} + 2D_{66}) \dfrac{\partial^4 w_1(x,y;t)}{\partial x^2 \partial y^2} + D_{22} \dfrac{\partial^4 w_1(x,y;t)}{\partial y^4} + \\ m_1^* \dfrac{\partial^2 w_1}{\partial t^2} - j\omega\rho_0 \Phi_1 - \sigma_z^s - \sigma_z^f \end{array} \right) .\varphi_{mn}(x,y) dxdy = 0 \tag{23}$$

$$\int_0^b \int_0^a \left(\begin{array}{l} D_{11} \dfrac{\partial^4 w_2(x,y;t)}{\partial x^4} + 2(D_{12} + 2D_{66}) \dfrac{\partial^4 w_2(x,y;t)}{\partial x^2 \partial y^2} + D_{22} \dfrac{\partial^4 w_2(x,y;t)}{\partial y^4} + \\ m_2^* \dfrac{\partial^2 w_2}{\partial t^2} + j\omega\rho_0 \Phi_3 + \sigma_z^s + \sigma_z^f \end{array} \right) .\varphi_{mn}(x,y) dxdy = 0 \tag{24}$$

To solve the entire problem numerically, a truncation is needed: $1 \le m, n \le N_{\max}$, where the choice of N_{max} is a trade-off between accuracy and computation cost. Substituting Eqs. (13), (16), (17) and the $\sigma_z^s; \sigma_z^f$ expressions into Eqs. (23) and (24) yields a N_{max} x N_{max} system. Once this matrix equation is solved, the unknowns $\alpha_{i,mn}$ ($i = 1, 2$) are determined. Consequently, all the variables dependent on $\alpha_{1,mn}$ and $\alpha_{2,mn}$ including β, γ, σ_z^s and σ_z^f will be completely resolved.

3. NUMERICAL RESULTS AND DISCUSSION

3.1. Validation of the present study

3.1.1. Double-aluminium plate with air cavity

For validation, the present analytical solutions are compared with the experimental results of Lu and Xin [7], as shown in Fig. 3. The double-plate considered consists of two identical aluminum (isotropic) faceplates. The dimensions of the plates are: length of the plate a = 0.3 m, width of the plate b = 0.3 m. The plate has thickness h = 0.001 m while the thickness of the air cavity is H = 0.08 m. The mechanical properties of aluminum materials are: E = 70 GPa; ρ = 2700 kg/m^3; v = 0.33. The airspeed of sound, c = 343 m/s; ρ_0 = 1.21 kg/m^3; the amplitude of the acoustic velocity potential for the incident sound is I_0 = 1 m^2/s.

Looking at Figure 3, we can see that the current predictions are closely matched with the experimental measurements of Xin *et al*. [7]. The obvious difference between theory and experiment is attributed to a number of factors such as the incident wave has not satisfied the condition of a plane wave or the connection of the structure or due to interference between waves during the experiment. Note also that the experimental results at frequencies below 100 Hz are not reliable because the flanking transmission paths of the test facility play a prominent role in this frequency range. The results of Fig. 3 clearly demonstrate the intense peaks and dips in the sound transmission loss versus frequency curve reflect the inherent modal behaviors of the double-plate system.

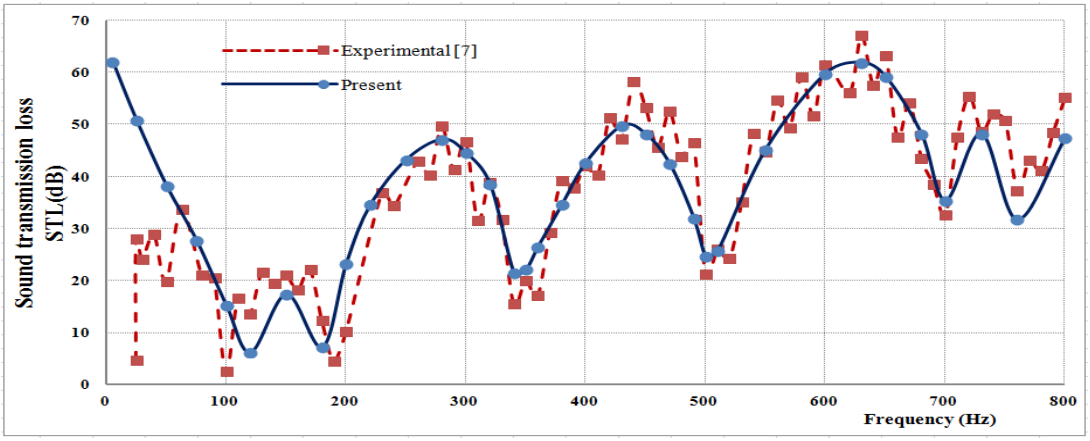

Figure 3. Comparison between the present prediction with the experimental result of [7].

3.1.2. Double-aluminium plate with porous layer

For the second validation test, the STL across a finite double-aluminium plate with poroelastic material is calculated and compared with theoretical result of Bolton *et al*. [1]. The property parameters of aluminium plates and poroelastic material are presented in Table 1.

It is obvious from Figure 4 that there is an acceptable agreement between present analytical and theoretical results shown in [1].

Table1 . Property parameters of the double aluminium plate and the poroelastic material.

Parameter	Symbol	Value
The double aluminium plate		
Young's moduluas	E_p	70 GPa
Bulk density	ρ_p	2700 kg/m^3
Poisson's ratio	v_p	0.33
Upper plate thickness	h_1	1.27 mm
Bottom plate thickness	h_2	0.762 mm
Length x width of plate	a x b	1.2 m x 1.2 m
Porous layer thikness	H	27 mm
The poroelastic material		
Bulk density of the solid phase	ρ_1	30 kg/m^3
In vacuo bulk Young's modulus	E_s	8.10^5 Pa
Bulk Poisson's ratio	v_s	0.40
Flow resistivity	ψ	25.10^3 MKS Rayls m^{-1}
Porosity	β	0.9
Geometrical structure factor	ϑ	0.78
Ratio of specific heats	χ	1.4
Prandtl number	Pr	0.71

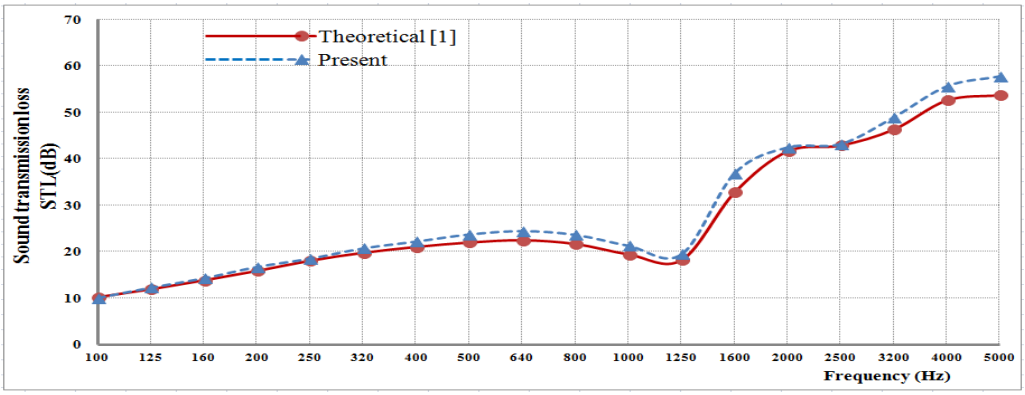

Figure 4. Comparison of sound transmission loss between the current study and theoretical result of Bolton *et al.* [1] for the double-aluminium plate with poroelastic material.

3.2. Influence of composite materials on STL

The influence of composite materials on STL through a finite clamped double-composite plate lined with poroelastic material is studied in this section by selecting four types of composite materials: Boron/Epoxy, Glass/Epoxy, Graphite/Epoxy and Kevlar/Epoxy. The double-plate consists of two identical orthotropic laminated composite faceplates. Laminate configuration of the bottom and the upper plate is $[0/90/0/90]_s$. The mechanical properties of composite material are shown in Table 2.

Table 2. Composite materials properties and the geometrical dimensions.

Composite	E_1 *(GPa)*	E_2 *(GPa)*	G_{12} *(GPa)*	ν_{12}	ρ *(kg/m^3)*	*a x b* *(m^2)*	h_1 *(mm)*	h_2 *(mm)*	*H (mm)*
Boron/Epoxy	204.000	18.500	5.590	0.23	2000	1.2 x 1.2	1.27	0.762	27
Glass/Epoxy	40.851	10.097	3.788	0.27	1946				
Graphite/Epoxy	181.000	10.300	7.170	0.28	1600				
Kevlar/Epoxy	76.000	5.500	2.300	0.34	1460				

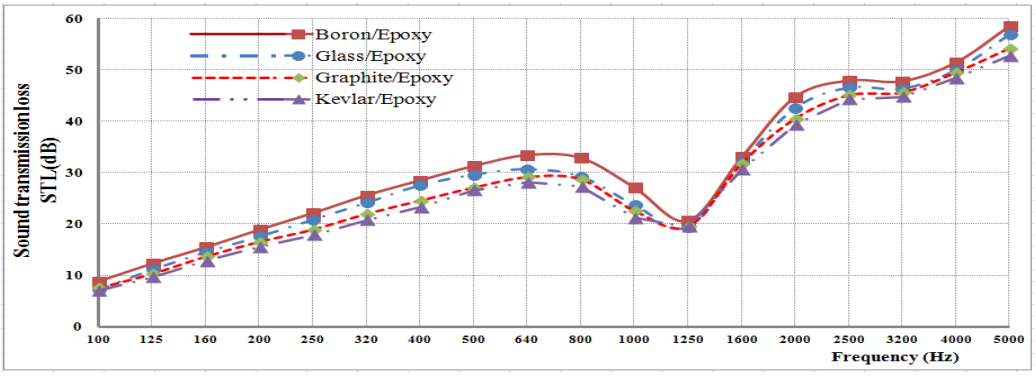

Figure 5. Influence of composite materials on STL of a clamped double-composite plate lined with poroelastic materials.

It is readily seen that, as a result of the density of the materials, the STL curves are ascending. Hence, the Boron/Epoxy and Glass/epoxy materials demonstrate a better transmission loss due to the densities that are greater than the other two materials.

3.3. Influence of lamination scheme on STL

In order to quantify the effects of lamination scheme on STL through the double-composite plate lined with poroelastic materials, four following configurations of the bottom and upper Glass/epoxy laminated composite plates are selected: $[0/90/0/90]_s$, $[0/0/0/0]_s$, $[90/90/90/90]_s$ and $[90/0/0/90]_s$. The geometrical and material parameters are shown in the Table 2.

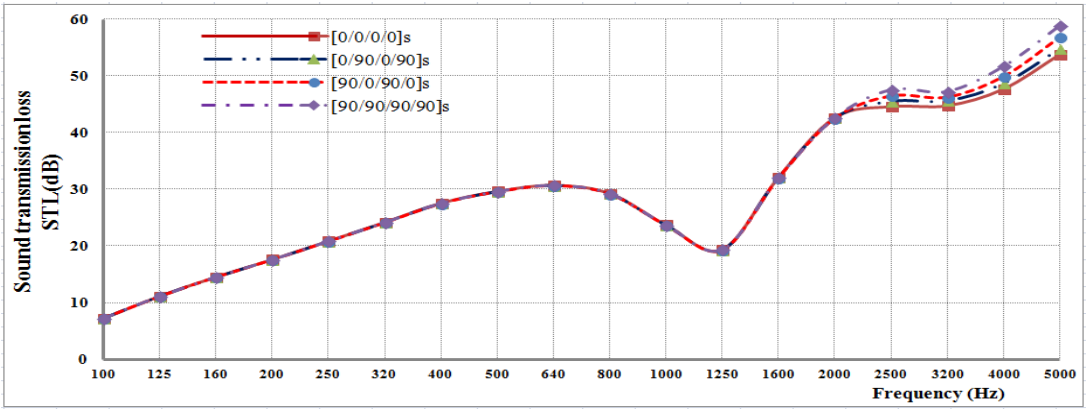

Figure 6. Influence of laminate configuration on STL of a clamped double-Glass/epoxy plate lined with poroelastic materials.

From Fig. 6, we see that, at frequencies below 2000 Hz, the seemingly identical curves show that the configuration change does not seem to affect the STL value, particularly at low frequencies. At frequencies above 2000 Hz, the plies arrangement $[90/90/90/90]_S$ has enhanced the structural STL more than the other options, particularly at higher frequencies.

3.4. Effect of density of porous material on STL

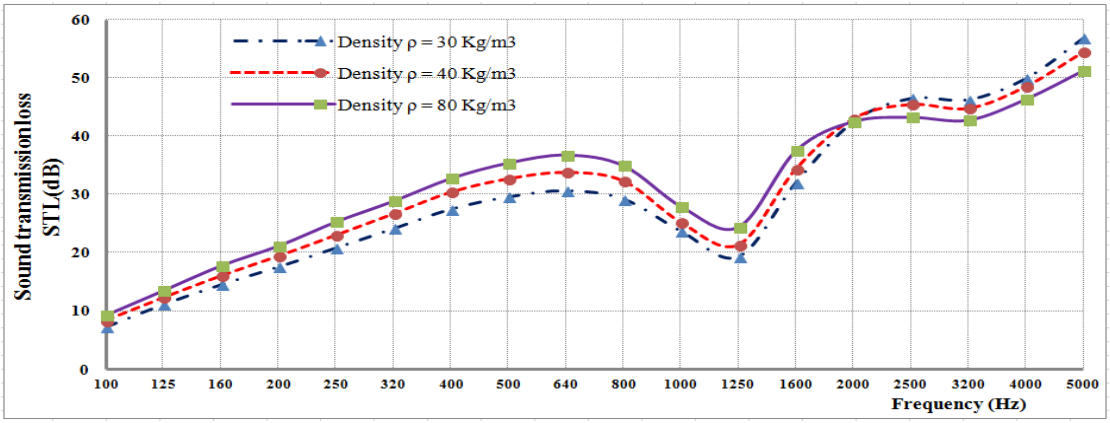

Figure 7. Effect of porous material density on STL.

Figure 7 shows the effect of porous core layer density (solid phase) on STL of the double-walled composite plate.

It is well observed that, in low frequency ranges, increasing the density of core layer improves the TL. However, in high frequencies it significantly reduces the TL.

4. CONCLUSIONS

An analytical approach has been developed to study the vibroacoustic behavior and the sound transmission loss across a clamped orthotropic laminated double-composite plate filled with porous materials. We get some of the following conclusions:

- The present predictions of STL are in good agreement with existing experimental results.
- The surface density of composite materials influences considerably on STL of finite clamped double-composite plate lined with porous materials.
- For the Glass/epoxy double-composite plate with porous cores, the plies being arranged in a $[90/90/90/90]_s$ pattern of the bottom and upper plates appear to outperform other considered lamination schemes in terms of sound insulation.
- As the density of the core layer increases, the sound insulation capacity of the double-composite plate also increases but at high frequencies it significantly reduces the TL.

Acknowledgements. This research is funded by Vietnam National Foundation for Science and Technology Development (NAFOSTED) under grant number: 107.02-2018.07.

REFERENCES

1. Bolton J. S., Shiau N. M. and Kang Y. J. - Sound transmission through multi-panel structures lined with elastic porous materials, Journal of Sound and Vibration **191** (3) (1996) 317-347.
2. Biot M. A. - Theory of propagation of elastic waves in a fluid-structural porous solid I: Low frequency range. Journal of the Acoustical Society of America **28** (2) (1956) 168-178.
3. Lee J. H., Kim J. and Kim H. J. - Simplified method to solve sound transmission through structures lined with elastic porous material, The Journal of the Acoustical Society of America **110** (5) (2001) 2282-2294.
4. Leppington F. G., Broadbent E. G. and Butler G. F. - Transmission of sound through a pair of rectangular elastic plates, IMA Journal of Applied Mathematics **71** (2006) 940–955.
5. Chazot J. D. and Guyader J. L. - Prediction of transmission loss of double panels with a patch mobility method, Journal of the Acoustical Society of America **121** (2007) 267–278.
6. Xin F. X. and Lu T. J. - Analytical and experimental investigation on transmission loss of clamped double panels: Implication of boundary effects, Journal of the Acoustical Society of America **125** (3) (2009) 1506–1517.
7. Lu T. J and Xin F. X. - Vibro-acoustics of Lightweight Sandwich, Science Press Beijing and Springer-Verlag Berlin Heidenberg (2014).

8. Thanh P. N. and Thinh T. I. – Sound transmission loss across a finite simply supported double-laminated composite plate with enclosed air cavity, Vietnam Journal of Science and Technology **57** (6) (2019) 749-761.
9. Panneton R. N. and Atalla N. - Numerical prediction of sound transmission through finite multilayer systems with poroelastic materials, J. Acoust. Soc. Am. **100** (1996) 346-354.
10. Leissa A. W. - Vibration of plates, Acoustical Society of America, New York (1993).
11. Frampton K. D. - The effect of flow-induced coupling on sound radiation from convected fluid loaded plates, J. Acoust. Soc. Am. **117** (2005) 1129–1137.